Inorganic Chemistry

Article

pubs.acs.org/IC

Tuning of Redox Potentials by Introducing a Cyclometalated Bond to Bis-tridentate Ruthenium(II) Complexes Bearing Bis(*N*-methylbenzimidazolyl)benzene or -pyridine Ligands

Wen-Wen Yang,[†] Yu-Wu Zhong,*[,†] Shinpei Yoshikawa,[‡] Jiang-Yang Shao,[†] Shigeyuki Masaoka,[§] Ken Sakai,[§] Jiannian Yao,[†] and Masa-aki Haga*[,‡]

[†]Beijing National Laboratory for Molecular Sciences, CAS Key Laboratory of Photochemistry, Institute of Chemistry, Chinese Academy of Sciences, Beijing 100190, People's Republic of China

[‡]Department of Applied Chemistry, Faculty of Science and Engineering, Chuo University, 1-13-27 Kasuga, Bunkyo-ku, Tokyo 112-8551, Japan

[§]Department of Chemistry, Faculty of Science, Kyushu University, Hakozaki 6-10-1, Higashi-ku, Fukuoka 812-8581, Japan

Supporting Information

ABSTRACT: A series of asymmetrical bis-tridentate cyclometalated complexes including $[Ru(Mebib)(Mebip)]^+$, $[Ru(Mebip)(dpb)]^+$, $[Ru(Mebip)(Medpb)]^+$, and $[Ru(Mebib)(tpy)]^+$ and two bis-tridentate noncyclometalated complexes $[Ru(Mebip)_2]^{2+}$ and $[Ru(Mebip)(tpy)]^{2+}$ were prepared and characterized, where Mebib is bis(*N*-methylbenzimidazolyl)-benzene, Mebip is bis(*N*-methylbenzimidazolyl)pyridine, dpb is 1,3-di-2-pyridylbenzene, Medpb is 4,6-dimethyl-1,3-di-2-pyridylbenzene, and tpy is 2,2′:6′,2″-terpyridine. The solid-state structure of $[Ru(Mebip)(Medpb)]^+$ is studied by X-ray crystallographic analysis. The electrochemical and spectroscopic properties of these ruthenium complexes were studied and compared with those of known complexes $[Ru(tpy)(dpb)]^+$ and $[Ru(tpy)_2]^{2+}$. The change of the supporting ligands and coordination environment allows progressive modulation of the metal-associated redox potentials ($Ru^{II/III}$) from +0.26 to +1.32 V vs Ag/AgCl. The introduction of a ruthenium cyclometalated bond in these complexes results in a significant negative potential shift. The $Ru^{II/III}$ potentials of these complexes were analyzed on the basis of Lever's electrochemical parameters (E_L). Density functional theory (DFT) and time-dependent DFT calculations were carried out to elucidate the electronic structures and spectroscopic spectra of complexes with Mebib or Mebip ligands.

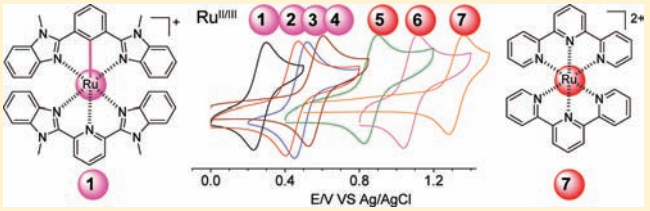

INTRODUCTION

Polyazine transition-metal complexes, particularly ruthenium(II) complexes, have attracted tremendous interest because of their distinguished electrochemical and photophysical properties.[1] They intensely absorb visible light from the metal-to-ligand charge-transfer (MLCT) transitions, which makes them good candidates as light-harvesting dyes and sensitizers.[2] Some ruthenium complexes with bright emission and long excited-state lifetimes, e.g., $[Ru(bpy)_3]^{2+}$ (bpy = 2,2′-bipyridine; Φ = 9.5% in oxygen-free acetonitrile; τ = 1150 ns),[3] are benchmark emissive organometallic complexes. They have been widely used in photoinduced electron- or energy-transfer processes and photocatalysis.[4] Bis-tridentate octahedral complexes such as $[Ru(tpy)_2]^{2+}$ (tpy = 2,2′:6′,2″-terpyridine) can be readily incorporated into supramolecular architectures with well-defined structures via easy and reliable functionalization at the 4′ position of the tpy ligand,[5] and linear multimetallic coordination arrays as potential molecular wires could be produced. However, it should be noted that the coordination environment and nature of the supporting ligands play significant roles in determining the electrochemical and photophysical properties of these complexes. This, in turn, determines their suitability for specific applications such as biomediators for electron shuttles between active sites of oxidoreductases and the electrode.[6]

Recently, cyclometalated ruthenium complexes have been the focus of many research activities.[7] These complexes contain a covalent Ru−C bond between the metal center and one supporting ligand. Because of the presence of the anionic cyclometalating ligand, the metal center of cyclometalated complexes is much more electron-rich than that of non-cyclometalated analogues. As a result, the metal-associated redox potentials of these complexes are much less positive than the noncyclometalated ones. For example, the $Ru^{II/III}$ process[8] of noncyclometalated complex $[Ru(tpy)_2]^{2+}$ occurs at +0.89 V vs Fc/Fc^+ (+1.3 V vs Ag/AgCl[9]), while this process could take place around at +0.12 V vs Fc/Fc^+ (corresponding to +0.57 V vs Ag/AgCl) for the cyclometalated analogue $[Ru(tpy)(dpb)]^+$ (dpb = 1,3-di-2-pyridylbenzene).[8] In this context, we also note that bis(triazole)- or bis(tetrazole)pyridine, as reported by Vos and co-workers, could also act as σ-donor ligands, and

Received: August 3, 2011
Published: December 28, 2011

   dx.doi.org/10.1021/ic2016885 | *Inorg. Chem.* 2012, 51, 890−899

Scheme 1. Synthesis of Compounds Studied

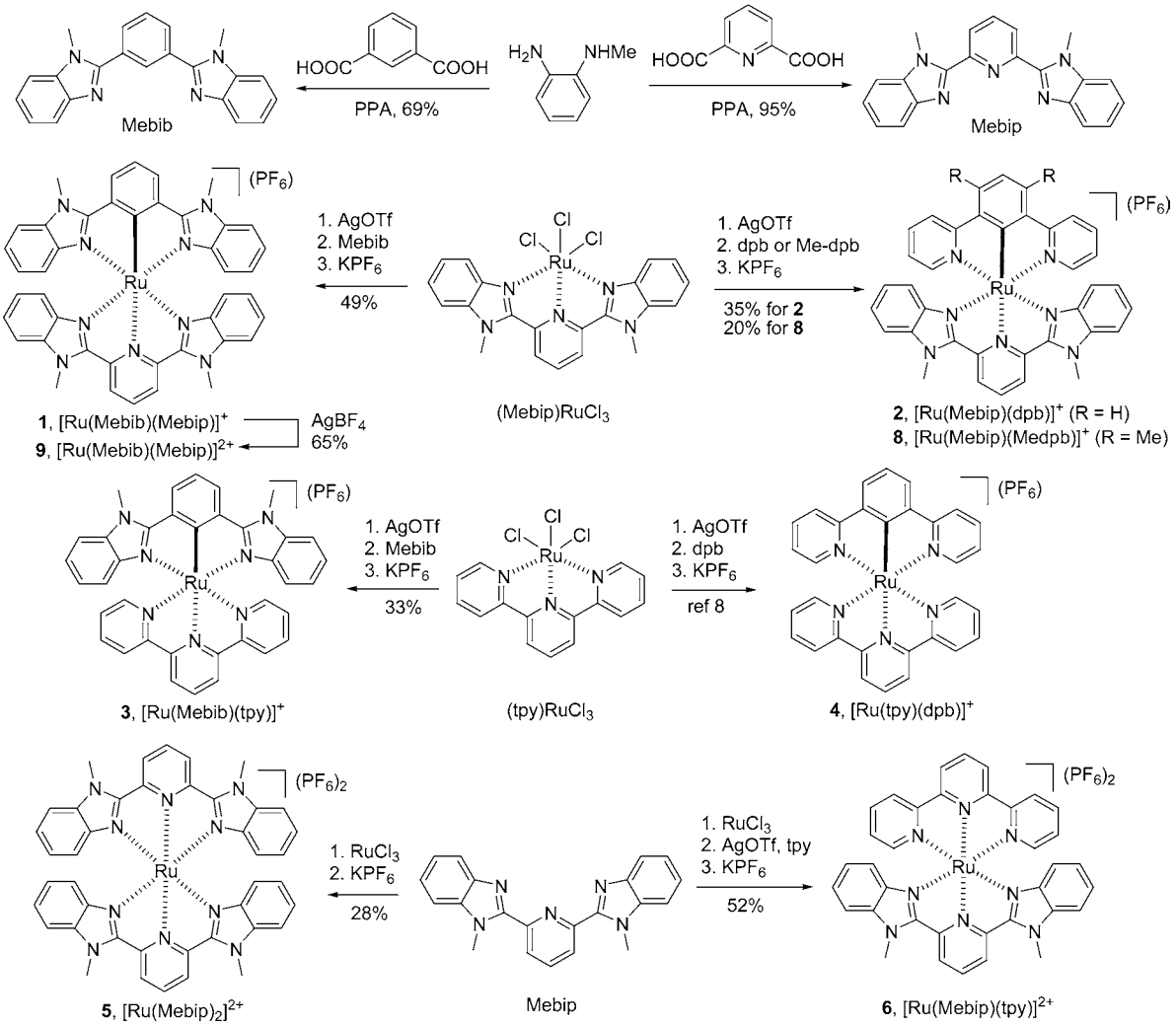

corresponding Ru^{II}(tpy)-type complexes show appealing emissive properties.[10] Recent investigations have proved that cyclometalated ruthenium complexes could be used as efficient sensitizers for solar cell applications,[11] benefiting from the energetic match between the metal-based highest occupied molecular orbital (HOMO) level of the dye and the conduction band edge of TiO_2. Besides, numerous mixed-valence systems with cyclometalated ruthenium as the charge-bearing sites have been reported and an enhanced electronic coupling between metal centers was found to be present.[12] Encouraged by their interesting properties and promising application in dye-sensitized solar cells and molecular electronics, we recently set out to design and synthesize new cyclometalated ruthenium complexes.[13] A cyclometalating tridentate ligand 1,3-di-1,2,3-triazol-4-ylbenzene (dtab) has previously been reported,[14] and corresponding complexes $[Ru(tpy)(dtab)]^+$ were found to exhibit electrochemical and spectroscopic properties similar to those of $[Ru(tpy)(dpb)]^+$. In this paper, we describe the synthesis and characterization of new cyclometalated ruthenium complexes $[Ru(Mebib)(Mebip)]^+$, $[Ru(Mebip)(dpb)]^+$, $[Ru(Mebip)(Medpb)]^+$, and $[Ru(Mebib)(tpy)]^+$, where Mebib is bis(*N*-methylbenzimidazolyl)benzene, Mebip is bis(*N*-methylbenzimidazolyl)pyridine, and Medpb is 4,6-dimethyl-1,3-di-2-pyridylbenzene. The electrochemical and photophysical properties of these complexes were studied and compared with those of $[Ru(tpy)(dpb)]^+$, $[Ru(Mebip)(tpy)]^{2+}$, $[Ru(Mebip)_2]^{2+}$, and $[Ru(tpy)_2]^{2+}$. In addition, density functional theory (DFT) and time-dependent DFT (TDDFT) calculations were performed on these complexes to elucidate their electronic structures and aid in the assignment of absorption spectra. The presence of strong electron-donating benzimidazole rings is believed to substantially decrease the redox potential of ruthenium complexes. The combination of cyclometalated and noncyclometalated ruthenium complexes with Mebib and Mebip would allow systematic tuning of the metal-centered redox potentials.

It should be noted that the coordination chemistry of Mebib and Mebip and their derivatives is well documented. For instance, Haga and co-workers have prepared a large number of noncyclometalated ruthenium and cyclometalated iridium complexes with Mebib and/or Mebip ligands and studied the properties of these complexes both in solution and on the electrode surface.[15] The reaction of Mebib and $Pd(OAc)_2$ was found to give a cyclometalated palladium(II) complex where Mebib behaved as a cyclometalating bidentate ligand.[16] In addition, copper(I),[17] platinum(II),[18] rhodium(III),[19] and lanthanide[20] complexes of Mebip or derivatives have been reported to form stable coordination complexes with appealing emissive or liquid-crystalline properties. It should also be mentioned that some Mebip- or Mebib-containing ruthenium

dx.doi.org/10.1021/ic2016885 | *Inorg. Chem.* 2012, 51, 890−899

complexes were successfully used as solar cell sensitizers or water oxidation catalysts recently.[21] However, cyclometalated ruthenium complexes with either Mebib or Mebip ligands have rarely been reported.[21d]

RESULTS AND DISCUSSION

Synthesis and X-ray Structure. The complexes studied in the paper were synthesized as outlined in Scheme 1. Detailed synthetic procedures and characterization data are provided in the Experimental Section. Ligands Mebib and Mebip were prepared according to reported procedures with slight modifications from the condensation of *N*-methyl-1,2-phenylenediamine with benzene-1,3-dicarboxylic acid and pyridine-2,6-dicarboxylic acid, respectively.[15f,21b] The reaction of $RuCl_3$ with Mebip afforded (Mebip)$RuCl_3$ in good yield,[21b] which was used as a common intermediate for the synthesis of asymmetric complexes **1**, **2**, **6**, and **8**. The chloride atoms of (Mebip)$RuCl_3$ were first replaced with solvent molecules (acetone in this case) in the presence of AgOTf. The obtained intermediate was heated in indicated solvents in the presence of Mebib, dpb, or Medpb to give cyclometalated complexes **1**, **2**, and **8**, respectively, after anion exchange with KPF_6. Similar procedures were previously used for the synthesis of a number of cyclometalated ruthenium complexes.[7,11−14] The reaction of (tpy)$RuCl_3$ and Mebib provided complex **3** in 33% yield. Known cyclometalated complex **4**[8] was also prepared for a comparison study. Two noncyclometalated complexes, **5** and **6**, could be prepared starting from Mebip. Complex **5** has been reported in the literature.[22] However, full characterization data are not available. Complex **6** is a new compound. However, it should be noted that similar complexes with substituents on the tpy ligand are known.[15]

Suitable single crystals of $[Ru(Mebip)(Medpb)]^+$ (**8**) with a BPh_4^- counteranion for structure determination were obtained by recrystallization from an acetonitrile−water solution. An ORTEP plot of **8** is represented in Figure 1. Crystal data and

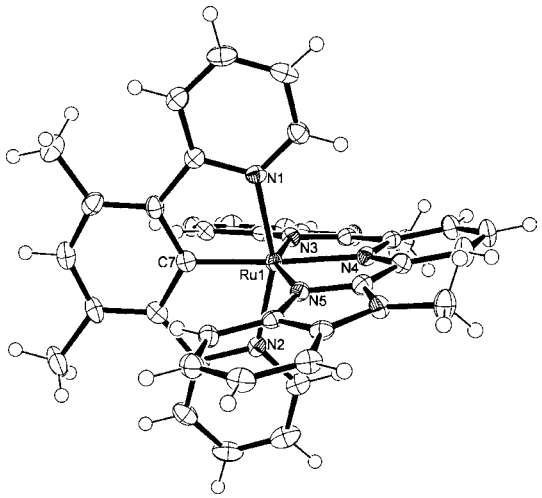

Figure 1. ORTEP diagram of **8** with a BPh_4^- counteranion. Solvents and anion are omitted for clarity.

selected bond lengths are given in Tables 1 and 2, respectively. The Medpb ligand binds to ruthenium in a tridentate N^C^N coordination mode with a covalent Ru−C bond. The coordination geometry of the ruthenim(II) center was a distorted octahedron. The Mebip ligand was not planar,

Table 1. Crystal Data and Structure Refinement for 8

$[Ru(Mebip)(Medpb)](BPh_4)CH_3CN$ (**8**)	
empirical formula	$C_{39}H_{32}RuN_7{\cdot}C_{24}H_{20}B{\cdot}C_2H_3N$
fw	1060.05
crystal color, habit	red, needle
cryst dimens	0.30 × 0.03 × 0.01 mm^3
cryst syst	orthorhombic
a (Å)	17.0541(19)
b (Å)	14.2024(15)
c (Å)	20.996(2)
V (Å^3)	5085.5(10)
space group	$Pca2_1$
Z value	4
D_{calc} (g/cm^3)	1.385
F_{000}	2200
R1[a] [$I > 2.00\sigma(I)$]	0.0383
wR2[b]	0.0771
GOF[c]	1.007

[a]$R1 = \sum||F_o| - |F_c||/|F_o|$. [b]$wR2 = [\sum w(|F_o|^2 - |F_c|^2)]^2/\sum w(|F_o|^2)^2]^{1/2}$. [c]$GOF = [\sum w(|F_o| - |F_c|)^2/(N_o - N_v)]^{1/2}$, where N_o = number of observations and N_v = number of variables.

Table 2. Selected Bond Lengths and Bond Angles of 8

bond lengths (Å)		bond angles (deg)	
Ru1−N1	2.066(3)	N1−Ru1−C7	79.2(1)
Ru1−N2	2.068 (3)	N2−Ru1−C7	79.0(1)
Ru1−N3	2.068(3)	N3−Ru1−N4	77.4(1)
Ru1−N4	2.055(3)	N4−Ru1−N5	76.5 (1)
Ru1−N5	2.075 (3)	N4−Ru1−C7	175.2 (1)
Ru1−C7	1.955(3)	N5−Ru1−C7	107.2 (1)

being slightly distorted because of repulsion between the *N*-methyl groups and the hydrogen atoms of the pyridine moiety. The Ru−C bond length is 1.955(3) Å. Bond lengths between ruthenium and coordinated nitrogen atoms are in the range of 2.066(3)−2.075(3) Å, except the Ru^{II}−$N4_{py}$ bond. The present Ru−$N4_{py}$ bond length is 2.055(3) Å, which is slightly longer than the values of 1.98−2.02 Å reported for Ru^{II}−N_{py} bond lengths in bis-tridentate $[Ru(tpy)_2]^{2+}$ and $[Ru(Mebip)_2]^{2+}$ complexes.[8] This result indicates that the trans influence of carbon anion coordination induces elongation of the Ru−$N4_{py}$ bond trans to the Ru−C7 bond.

Electrochemical Studies and DFT Calculation. The electronic properties of these complexes were studied by electrochemical analysis and compared with those of $[Ru(tpy)(dpb)]^+$ and $[Ru(tpy)_2]^{2+}$ (Figure 2 and Table 3). To assist in the determination of their electronic structures, DFT calculations were performed on the B3LYP/LANL2DZ level. Some frontier orbital structures with electron density distribution are provided in Figures 3 and S1−S4 in the Supporting Information. The frontier orbital energy level diagram for complexes **1**−**3**, **5**, and **6** is shown in Figure 4. The cyclic voltammetry (CV) profiles of cyclometalated complexes **1**−**3** show some similarities albeit with a distinct difference. All of them display a cathodic wave around −1.60 V vs Ag/AgCl and two anodic waves within the solvent potential window. The cathodic event is assigned to reduction of the noncyclometalating ligand Mebip for complexes **1** and **2** and tpy for complex **3**. The anionic cyclometalating ligand is more electron-rich and thus sluggish to be reduced than the noncyclometalating ligand. This assignment is corroborated

dx.doi.org/10.1021/ic2016885 | *Inorg. Chem.* 2012, 51, 890−899

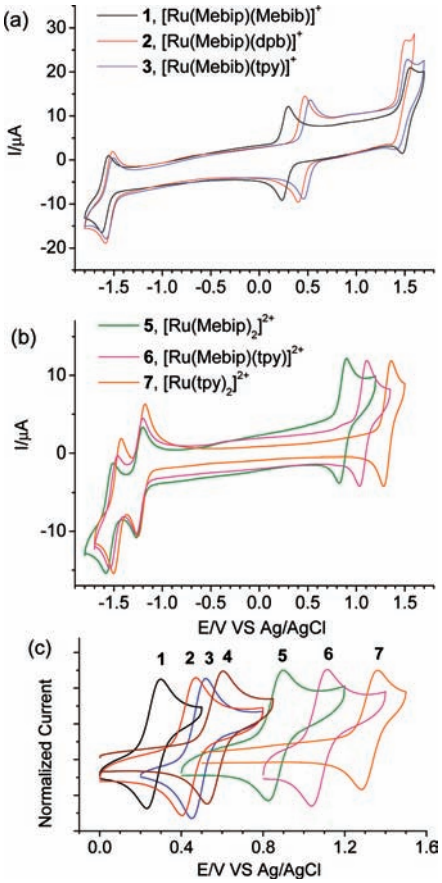

Figure 2. Cyclic voltammograms of **1**−**7** in acetonitrile containing 0.1 M Bu_4NClO_4 as the supporting electrolyte at a scan rate of 100 mV/s. The working electrode was a glassy carbon, the counter electrode was a platinum wire, and the reference electrode was Ag/AgCl in saturated aqueous NaCl.

by DFT calculations. The lowest unoccupied molecular orbitals (LUMOs) of complexes **1**−**3** are all predominantly associated with the noncyclometalating ligand (Figures 3 and S1 and S2 in the Supporting Information). The anodic events of complexes **1**−**3** are rather interesting. The first oxidation waves (+0.26, +0.43, and +0.48 V vs Ag/AgCl for complexes **1**−**3**, respectively) could be attributed to the mixed $Ru^{II/III}$/ligand oxidation process.[7,11−14] They are noticeably less positive than that of $[Ru(tpy)(dpb)]^+$ (**4**; +0.56 V vs Ag/AgCl). Complex **1** coordinated with four benzimidazole rings could be oxidized at the lowest potential. It should be pointed out here that the $Ru^{II/III}$ process must involve some degree of ligand-based oxidation. It is supported by the DFT results that the HOMOs of **2** and **3** and HOMO−1 of complex **1** exhibit high electron delocalization between ruthenium and the cyclometalating phenyl ring. This phenomenon is commonly observed in the DFT results of cyclometalated ruthenium complexes.[7,11] The second oxidation waves of complexes **1**−**3** at around +1.50 V are ascribed to the $Ru^{III/IV}$ process. Similarly, some content of ligand oxidation must be present in this process. Importantly, in the cases of complexes **1** and **3** (especially **1**), this process exhibits well-defined chemical reversibility. We note that this process is clearly irreversible for most known cyclometalated ruthenium complexes[7,11−14] except in those bonded to oligothiophenes, as reported by Wolf and co-workers.[7f] This again attests to the importance of benzimidazole ligands, which stabilize the higher oxidation state because of their stronger σ-donor nature than pyridines. Because of the considerably low $Ru^{II/III}$ potential of complex **1**, it could be easily transformed to ruthenium(III) complex **9** in the presence of silver salt. The characterization data of **9** are available in the Experimental Section.

The CV profiles of complexes **5**−**7** are given in Figure 2b. They all display two ligand-based reduction waves and a $Ru^{II/III}$ process. For the asymmetric complex **6**, the Mebip ligand is thought to be first reduced, as suggested by the DFT results (Figure S4 in the Supporting Information), which gives a Mebip-associated LUMO level and a tpy-based LUMO+1 level. The $Ru^{II/III}$ process of complexes **5**−**7** occurs at +0.86, +1.07, and +1.32 V vs Ag/AgCl, respectively. The significantly low $Ru^{II/III}$ potential of benzimidazole-containing noncyclometalated ruthenium complexes has been documented previously.[15] By taking together the $Ru^{II/III}$ processes of complexes **1**−**7**, we successfully realize the systematic regulation of the metal-based oxidation potential from +0.26 to +1.32 V vs Ag/AgCl (Figure 2c). Correspondingly, the HOMO levels of these complexes vary in a progressively descending order. We have carried out DFT calculations on five complexes, **1**−**3**, **5**, and **6**. Their HOMO levels are found to reside at −6.96, −7.15, −7.31, −10.00, and −10.50 eV, respectively (Figure 4). However, it should be pointed out we did not consider the compensation for counteranions during calculations. The relative energy level

Table 3. Observed and Calculated Electrochemical Data of Complexes 1−7

				number of ligand parts[a]					
complex	$E_{1/2}$[b] for $Ru^{II/III}$, $Ru^{III/IV}$	$E_{1/2}$[b] for $L^{0/-}$	ΔE[c] (eV)	py_{tpy}	py_{phenyl}	py_{bzim}	Ph anion	bzim	$E_{1/2}$(calcd)[b]
1, $[Ru(Mebib)(Mebip)]^+$	+0.26, +1.50	−1.60	1.86			1	1	4	+0.29
2, $[Ru(Mebip)(dpb)]^+$	+0.43, +1.49[d]	−1.56	1.92		2	1	1	2	+0.39
3, $[Ru(Mebib)(tpy)]^+$	+0.48, +1.47	−1.55	1.95	3			1	2	+0.49
4, $[Ru(tpy)(dpb)]^+$	+0.56, +1.60[d]	−1.51	2.07	3	2		1		+0.60
5, $[Ru(Mebip)_2]^{2+}$	+0.86	−1.24, −1.55	2.10			2		4	+0.87
6, $[Ru(Mebip)(tpy)]^{2+}$	+1.07	−1.24, −1.50	2.31	3		1		2	+1.07
7, $[Ru(tpy)_2]^{2+}$	+1.32	−1.22, −1.46	2.54	6					+1.27
8, $[Ru(Mebip)(Medpb)]^+$	+0.38, +1.57[d]	−1.57	1.95						

[a]The following Lever electrochemical parameters (V vs NHE) were used: py_{tpy} (pyridine of tpy) = 0.25, py_{phenyl} (pyridine with a adjacent phenyl group) = 0.23, py_{bzim} (pyridine with a adjacent benzimidazole group) = 0.20, Ph anion (carboanion) = −0.40, and bzim (bibenzimidazole) = 0.17. The potential values for $E_{1/2}$(calcd) (V vs Ag/AgCl) was obtained by subtracting 0.22 V from those vs NHE. [b]The potential is reported as the $E_{1/2}$ value vs Ag/AgCl. [c]The electrochemical energy gap is determined by the potential difference between the first oxidation and first reduction waves. [d]$E_{p,anodic}$, irreversible.

dx.doi.org/10.1021/ic2016885 | Inorg. Chem. 2012, 51, 890−899

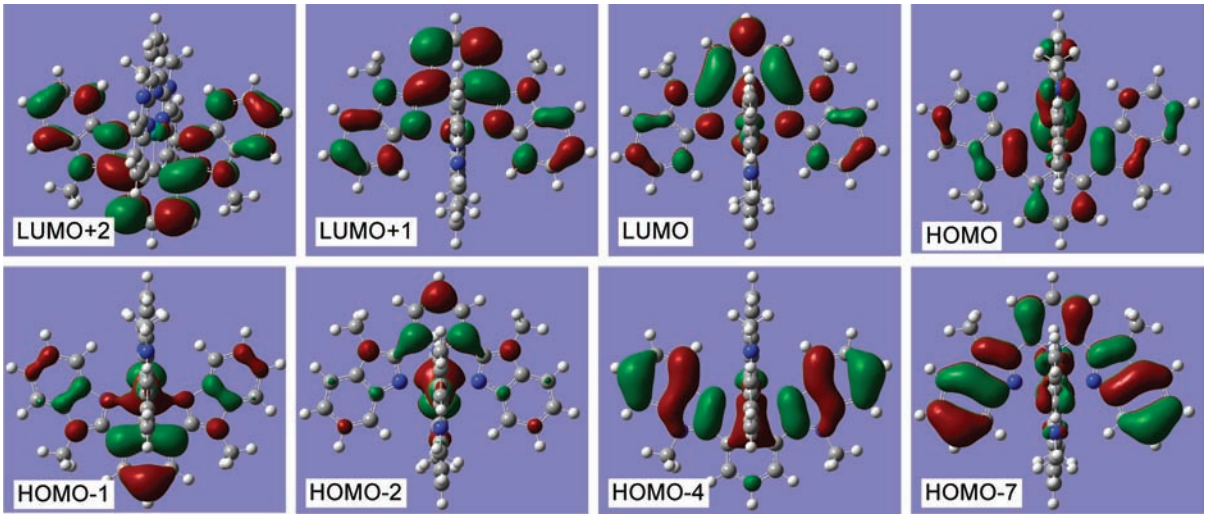

Figure 3. Isodensity plots of frontier orbitals of complex **1**. All orbitals have been computed at an isovalue of 0.02.

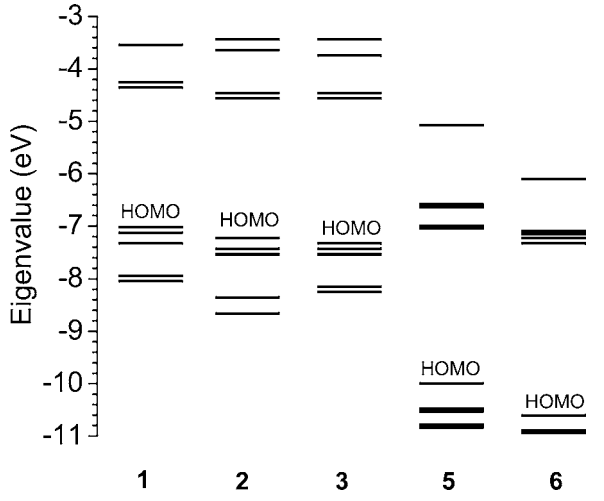

Figure 4. Frontier orbital energy level alignment of complexes **1**−**3**, **5**, and **6**.

difference between the cyclometalated and noncyclometalated series may be overestimated. It should also be noted that the energy gap of complexes **1**−**7**, determined by the potential difference between the first cathodic and first anodic waves, is varied in an ascending order from 1.86 to 2.54 eV (Table 3).

Lever's electrochemical parameter, E_L, has been used to predict $Ru^{II/III}$ redox potentials by assuming that all of the ligand contributions are additive.[23] For the observed $Ru^{II/III}$ couple in acetonitrile (V vs NHE), the following equation applies:

$$E_{obs} = 0.97[\sum E_L] + 0.04 \quad (1)$$

In the present study, we have prepared a series of cyclometalated and noncyclometalated ruthenium complexes bearing Mebib and/or Mebip ligands. By using the reported Lever's parameters for the nitrogen-coordinating ligands such as the pyridine (0.25 for tpy and 0.20 for benzimidazole) or benzimidazole ligand (0.17 for bibenzimdazole) and eq 1, we can derive the electrochemical parameter for the phenyl anion in ruthenium cyclometalated complexes as −0.40. The predicted $E_{1/2}$ values are listed in Table 3, together with the experimental values. The large negative value of E_L for the phenyl anion indicates that the phenyl anion of the cyclometalated bond acts as a strong π base.

Spectroscopic Studies and TDDFT Calculation. The UV/vis absorption spectra of the above compounds were recorded (Figures 5 and S5 in the Supporting Information) to further probe their electronic properties. To aid in the assignment of absorption bands, TDDFT calculations were performed on these complexes, and related results are collected in Table 4, together with experimentally observed transitions. Predicted absorption spectra are provided in Figure S6 in the Supporting Information. It is well-known that polypyridine ruthenium complexes display strong intraligand (IL) absorptions in the UV region and MLCT transitions in the visible region.[1,2] One common feature for the complexes studied is that, for complexes with the Mebip ligand, no matter cyclometalated (**1** and **2**) or noncyclometalated (**5** and **6**), intense Mebip-based IL transitions could be observed around

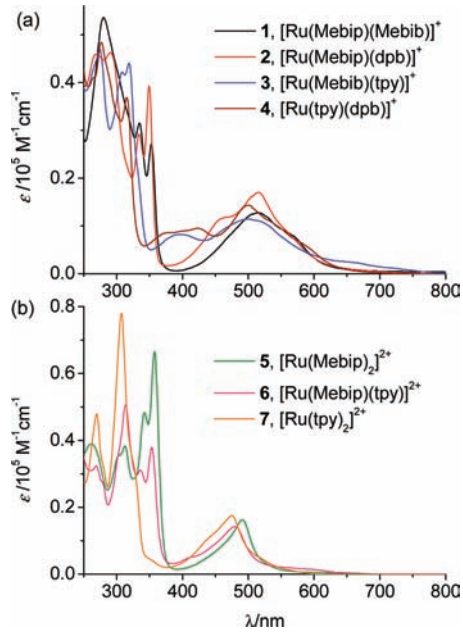

Figure 5. UV/vis absorption spectra of complexes **1**−**7** in acetonitrile.

dx.doi.org/10.1021/ic2016885 | *Inorg. Chem.* 2012, 51, 890−899

Table 4. Observed Absorption Data and Calculated Excitation Energy (E), Oscillator Strength (f), Dominant Contributing Transitions, and the Associated Percent Contribution and Assignment of Complexes 1−3, 5, and 6[a]

complex	S_n	E/eV	E/nm	f	λ_{max}/nm obsd	ε ($\times 10^5$ M^{-1} cm^{-1})	dominant transitions (percent contribution[b])	assignment
1	6	2.65	468	0.101	571	0.077	HOMO−2 → LUMO (58%)	$ML_{Mebip}CT$
	8	2.89	428	0.151	515	0.13	HOMO−1 → LUMO+2 (91%)	$ML_{Mebib}CT$
	23	3.65	339	0.181	353	0.27	HOMO−7 → LUMO (89%)	IL_{Mebip}
	27	3.84	322	0.213	334	0.32	HOMO−8 → LUMO+1 (86%)	IL_{Mebip}
	30	3.92	315	0.177			HOMO−4 → LUMO+2 (82%)	IL_{Mebib}
2	6	2.71	458	0.139	516	0.17	HOMO−2 → LUMO (44%)	$ML_{Mebip}CT$
							HOMO−1 → LUMO+1 (23%)	$ML_{Mebip}CT$
	7	2.84	436	0.072	457	0.115	HOMO → LUMO+2 (84%)	$ML_{dpb}CT$
	11	3.18	390	0.086			HOMO−1 → LUMO+3 (76%)	$ML_{dpb}CT$
	18	3.57	347	0.239	349	0.39	HOMO−4 → LUMO (88%)	IL_{Mebip}
	24	3.79	327	0.12	334	0.29	HOMO−5 → LUMO+1 (72%)	IL_{Mebip}
3	6	2.59	478	0.069			HOMO−2 → LUMO (60%)	$ML_{tpy}CT$
	7	2.95	419	0.156	497	0.11	HOMO → LUMO+2 (90%)	$ML_{Mebib}CT$
	17	3.28	378	0.045	394	0.082	HOMO−1 → LUMO+3 (89%)	$ML_{tpy}CT$
	20	3.40	364	0.034			HOMO−1 → LUMO+4 (68%)	$ML_{tpy}CT$
	30	3.91	317	0.153	319	0.44	HOMO−4 → LUMO+2 (73%)	IL_{Mebib}
	37	4.17	297	0.168	275	0.47	HOMO−7 → LUMO (64%)	IL_{tpy}
5	4	2.52	491	0.016			HOMO → LUMO+3 (87%)	$ML_{Mebip}CT$
	7	2.84	437	0.094	491	0.16	HOMO−2 → LUMO (29%)	$ML_{Mebip}CT$
							HOMO−1 → LUMO+1 (29%)	$ML_{Mebip}CT$
	14	3.30	375	0.104	357	0.66	HOMO−3 → LUMO (92%)	IL_{Mebip}
	15	3.30	375	0.104			HOMO−3 → LUMO+1 (92%)	IL_{Mebip}
	16	3.39	365	0.14	342	0.48	HOMO−4 → LUMO (91%)	IL_{Mebip}
	17	3.39	365	0.14			HOMO−4 → LUMO+1 (91%)	IL_{Mebip}
6	7	2.91	425	0.12	480	0.14	HOMO−2 → LUMO+1 (50%)	$ML_{tpy}CT$
	9	3.01	411	0.019			HOMO−2 → LUMO+3 (76%)	$ML_{Mebip}CT$
	14	3.36	369	0.345	354	0.38	HOMO−3 → LUMO (84%)	IL_{Mebip}
	26	3.71	334	0.080			HOMO−4 → LUMO+3 (34%)	IL_{Mebip}
	31	3.86	321	0.18	336	0.31	HOMO−6 → LUMO+3 (83%)	IL_{Mebip}

[a]Computed at the TDDFT/LANL2DZ level of theory. [b]The actual percent contribution = (configuration coefficient)^2 × 2 × 100%.

350 nm (denoted as IL_{Mebip}, two sharp peaks). They originated from relatively high occupied levels, e.g., HOMO−4, HOMO−7, and HOMO−8 for complex **1** and HOMO−3, HOMO−4, and HOMO−6 for complex **6**. Transitions in the visible region for all complexes consist of MLCT bands associated with both coordinating ligands, either cyclometalated or noncyclometalated. Complex **1** shows $ML_{bip}CT$ and $ML_{bib}CT$ transitions at 571 and 515 nm, respectively. They are associated with excitation of HOMO−2 → LUMO and HOMO−1 → LUMO +2, respectively. In comparison, the Mebip- and dpb-targeted MLCT absorptions of complex **2** are found at 516 and 457 nm and dominated by HOMO−2 → LUMO and HOMO → LUMO+2 transitions, respectively. The absorption spectrum of **3** is somewhat similar to that of $[Ru(tpy)(dpb)]^+$. The major band around 500 nm is attributed to an admixture of both Mebib- and tpy-targeted MLCT transitions. However, $ML_{bib}CT$ transitions play a more important role, as predicted by TDDFT calculations. Transitions around 400 nm are assigned to the tpy-targeted MLCT bands. It should be noted that MLCT transitions of cyclometalated complexes (**1**−**4**) are relatively bathochromically shifted and more broadened than those of noncyclometalated complexes (**5**−**7**). This feature has been previously documented on cyclometalated ruthenium complexes.[11,12] Transitions at 480 nm of the asymmetric complex **6** contain MLCT transitions of both Mebip and tpy ligands. However, $ML_{tpy}CT$ has the major contribution. Finally, it is found that all complexes studied are weakly emissive or virtually nonemissive at room temperature in a fluidic solution.

The room-temperature emission spectra of complexes **3** and **6** in butyronitrile are shown in Figure 6. They weakly emit at 790

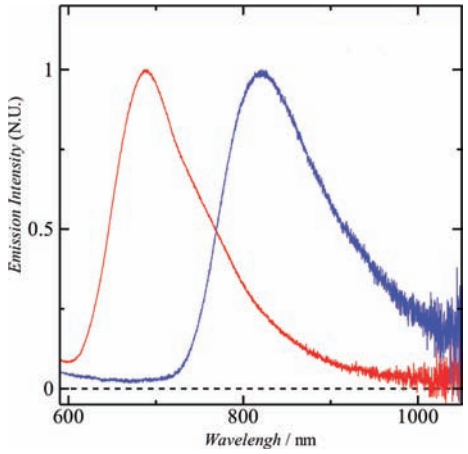

Figure 6. Emission spectra of complexes **3** (blue line) and **6** (red line) in butyronitrile at room temperature.

and 680 nm and have 16 and 30 ns lifetimes at room temperature, respectively. Compared to the emission properties of $[Ru(tpy)_2]^{2+}$ ($\lambda_{max,em}$ = 629 nm; τ = 0.25 ns) and $[Ru(L3)(tpy)]^0$ (L3 = 2,6-bis([1,2,3,4]tetrazol-5-yl)pyridine; $\lambda_{max,em}$ = 680 nm; τ = 42 ns) at room temperature,[10] the introduction of the Ru−C bond in complex **3** leads to a longer

dx.doi.org/10.1021/ic2016885 | Inorg. Chem. 2012, 51, 890−899

wavelength shift on emission. In order to get the information about the ^{3}MLCT−^{3}MC energy gap at the excited state, a detailed study for the temperature dependence of the luminescence lifetime is now underway, which will be published as a separate paper.

Oxidative Spectroelectrochemistry. Oxidative spectroelectrochemistry for the $Ru^{II/III}$ process was measured using a thin-layer spectroelectrochemical cell. The original ruthenium(II) complex **1**, $[Ru(Mebib)(Mebip)]^+$, shows several broad MLCT bands at 515 and 571 nm. The UV/vis spectral changes of the thin-layer spectroelectrochemical oxidative electrolysis of **1** at +0.5 V and then +1.6 V vs Ag/AgCl for the first and second oxidations are displayed in Figure 7. For the first

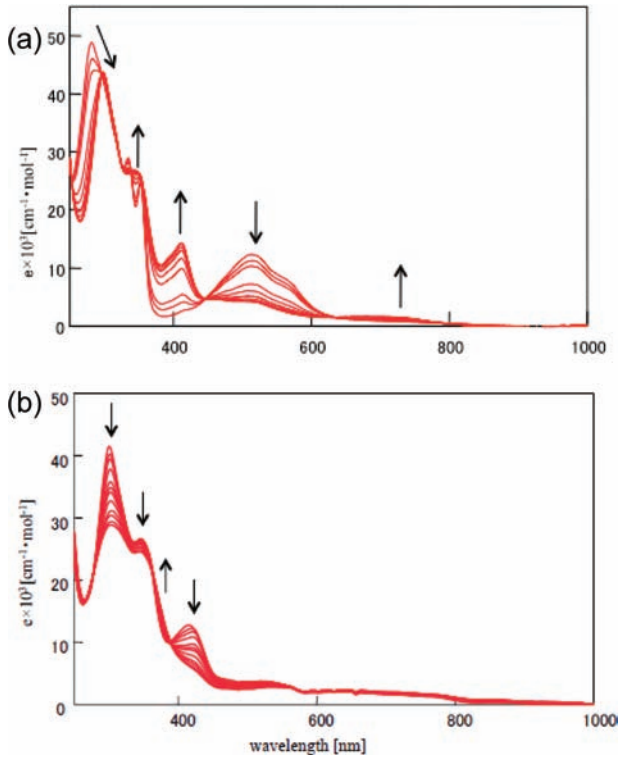

Figure 7. UV/vis spectral changes of complex **1** at applied potentials of +0.5 V (a) and +1.6 V (b) vs Ag/AgCl during oxidative thin-layer spectroelectrochemistry in 0.1 M $TBAPF_6$ in CH_3CN.

oxidation (Figure 7a), the disappearance of the MLCT bands at 515 nm and the appearance of new bands at 412 and 715 nm are clearly seen along with several isosbestic points at 297, 324, 339, 447, 637, and 790 nm. The latter band at 715 nm might be assigned to the ligand-to-metal charge-transfer band. The original $\pi\pi^*$ band at 281 nm was shifted to a longer wavelength at 299 nm after oxidation to the Ru^{III} state. From analysis of the Nernst plot, the number of electrons, n, and the standard oxidation potential, E°, were determined as n = 1 and E° = +0.24 V vs Ag/AgCl. The second oxidation led to a decrease of the band at 412 nm and the broadening of all of the bands and a small broad band appeared around 830 nm. Because ruthenium(IV) examples are rare except those of ruthenium(IV) oxo complexes,[24] no strong characteristic bands were observed. Similar spectral changes were observed for complexes **3** and **6** (Figure 8a,b). The trial to get the spectrum of the Ru^{IV} state for complex **3** has failed so far because of decomposition of the complex.

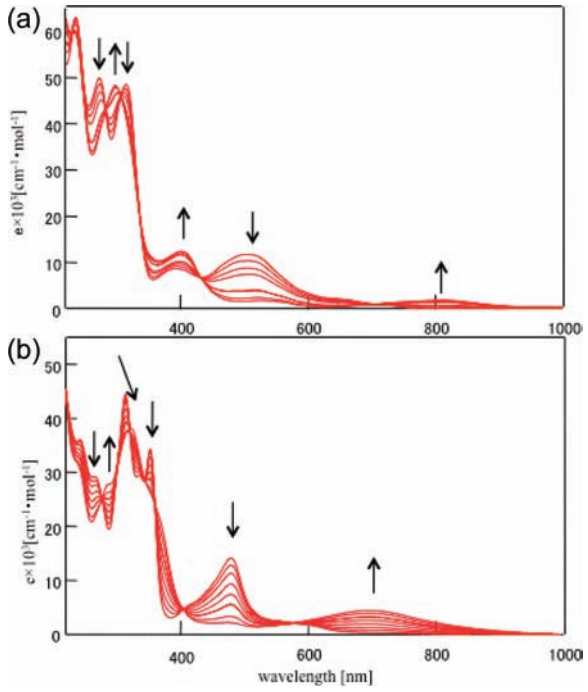

Figure 8. UV/vis spectral changes of complexes **3** (a) and **6** (b) during oxidative thin-layer spectroelectrochemistry in 0.1 M $TBAPF_6$ in CH_3CN.

CONCLUSION

In summary, a number of cyclometalated and noncyclometalated ruthenium complexes containing Mebip and/or Mebib ligands are presented in this paper. The electronic properties of these complexes were studied with electrochemical, spectroscopic, and spectroelectrochemical analysis and theoretical calculations. A key finding is that, by using benzimidazole-containing ligands, the metal-based oxidation potential of the corresponding ruthenium complexes could be systematically tuned in a wide scope (+0.26 to +1.32 V vs Ag/AgCl). As a result, HOMO levels and energy gaps of these complexes are varied in a controlled fashion. This feature is of importance and interest for the design and synthesis of new organometallic materials for applications in dye-sensitized solar cells.[11] We are currently carrying out the synthesis of new mixed-valent dimetallic systems with Mebip or Mebib ligands.[12−15] The presence of the electron-rich benzimidazole ligands is thought to greatly enhance the metal−metal coupling in these systems. These results will be reported in due course in the near future.

EXPERIMENTAL SECTION

General Procedure. NMR spectra were recorded in the designated solvent on a Bruker Avance 400 or 500 MHz spectrometer. Spectra are reported in ppm values from residual protons of a deuterated solvent for ^{1}H NMR. Mass spectrometry (MS) data were obtained with a Bruker Daltonics Inc. ApexII FT-ICR or Autoflex III MALDI-TOF mass spectrometer. Microanalysis was carried out using a Flash EA 1112 or Carlo Erba 1106 analyzer at the Institute of Chemistry, Chinese Academy of Sciences.

1,3-Bis(1-methylbenzimidazol-2-yl)benzene (Mebib). A mixture of isophthalic acid (680 mg, 4.1 mmol) and *N*-methyl-1,2-phenylenediamine (1.64 g, 8.4 mmol) in 20 mL of poly(phosphoric acid) was stirred at 210 °C for 4 h. After cooling to room temperature, the reaction mixture was poured into 50 mL of water and neutralized with 5 M aqueous NaOH. The precipitate was collected by filtration and washing with water. The resulting solid was subjected to flash

dx.doi.org/10.1021/ic2016885 | *Inorg. Chem.* 2012, 51, 890−899

column chromatography on silica gel (eluent: 4:1 CH_2Cl_2/acetone) to give 960 mg of Mebib as a yellow solid (69%). ^{1}H NMR (400 MHz, $CDCl_3$): δ 3.91 (s, 6H), 7.35 (m, 4H), 7.42 (d, J = 7.0 Hz, 2H), 7.71 (t, J = 7.8 Hz, 1H), 7.84 (d, J = 6.8 Hz, 2H), 7.93 (d, J = 7.6 Hz, 2H), 7.14 (s, 1H).

2,6-Bis(1-methylbenzimidazol-2-yl)pyridine (Mebip). A mixture of pyridine-2,6-dicarboxylic acid (0.68 g, 4.1 mmol) and *N*-methyl-1,2-phenylenediamine (1.73 g, 8.9 mmol) in 20 mL of poly(phosphoric acid) was stirred at 210 °C for 4 h. After cooling to room temperature, the reaction mixture was poured into 50 mL of water and neutralized with 5 M aqueous NaOH. The precipitate was collected by filtration and washing with water. The resulting solid was subjected to flash column chromatography on silica gel (eluent: 5:1 CH_2Cl_2/methanol) to give 1.31 g of Mebip as a yellow solid (95%). ^{1}H NMR (400 MHz, $CDCl_3$): δ 4.25 (s, 6H), 7.39 (m, 4H), 7.47 (d, J = 7.7 Hz, 2H), 7.88 (d, J = 7.5 Hz, 2H), 8.06 (t, J = 7.8 Hz, 1H), 8.42 (d, J = 7.8 Hz, 2H).

Complex 1. To 10 mL of dry acetone were added Ru(Mebip)Cl_3 (55 mg, 0.1 mmol) and AgOTf (78 mg, 0.3 mmol). The mixture was refluxed for 2 h before cooling to room temperature. The precipitate was removed by filtration, and the filtrate was concentrated to dryness. To the residue were added Mebib (33 mg, 0.1 mmol), *N*,*N*-dimethylformamide (DMF; 8 mL), and *tert*-butyl alcohol (*t*-BuOH; 8 mL). The mixture was then refluxed for 24 h. After cooling to room temperature, the solvent was removed under reduced pressure, and the residue was dissolved in the proper amount of methanol. After the addition of an excess of KPF_6, the resulting precipitate was collected by filtration and washing with water and Et_2O. The obtained solid was subjected to flash column chromatography on silica gel (eluent: 10:1 CH_2Cl_2/CH_3CN) to give 45 mg of complex **1** (49%). ^{1}H NMR (400 MHz, CD_3CN): δ 4.51 (s, br, 6H), 4.60 (s, br, 6H), 5.80 (m, br, 2H), 6.11 (d, J = 7.5 Hz, 2H), 6.76 (t, J = 7.5 Hz, 2H), 6.81 (t, J = 7.6 Hz, 2H), 6.93 (m, 2H), 7.13 (t, J = 7.7 Hz, 2H), 7.26 (d, J = 8.2 Hz, 2H), 7.36 (d, J = 8.3 Hz, 2H), 7.70 (t, J = 7.6 Hz, 1H), 8.15 (br, 2H), 8.40 (t, J = 7.4 Hz, 1H), 8.50 (br, 2H). ESI-MS: m/z 778.4 for $[M - PF_6]^+$. Anal. Calcd for $C_{43}H_{34}F_6N_9PRu{\cdot}H_2O$: C, 54.89; H, 3.86; N, 13.40. Found: C, 55.27; H, 3.66; N, 13.57.

Complex 2. To 10 mL of dry acetone were added Ru(Mebip)Cl_3 (55 mg, 0.1 mmol) and AgOTf (78 mg, 0.3 mmol). The mixture was refluxed for 2 h before cooling to room temperature. The precipitate was removed by filtration, and the filtrate was concentrated to dryness. To the residue were added 1,3-di-2-pyridylbenzene (23.2 mg, 0.1 mmol), DMF (8 mL), and *t*-BuOH (8 mL). The mixture was then refluxed for 24 h. After cooling to room temperature, the solvent was removed under reduced pressure, and the residue was dissolved in the proper amount of methanol. After the addition of an excess of KPF_6, the resulting precipitate was collected by filtration and washing with water and Et_2O. The obtained solid was subjected to flash column chromatography on silica gel (eluent: 10:1 CH_2Cl_2/CH_3CN) to give 28.5 mg of complex **2** (35%). ^{1}H NMR (400 MHz, CD_3CN): δ 4.38 (s, 6H), 6.06 (d, J = 8.2 Hz, 2H), 6.57 (t, J = 6.5 Hz, 2H), 6.81 (t, J = 7.7 Hz, 2H), 7.07 (d, J = 5.5 Hz, 2H), 7.22 (t, J = 7.7 Hz, 2H), 7.46 (m, overlapped, 4H), 7.61 (t, J = 7.6 Hz, 1H), 8.03 (d, J = 8.0 Hz, 2H), 8.21 (t, J = 8.1 Hz, 1H), 8.34 (d, J = 7.6 Hz, 2H), 8.75 (d, J = 8.1 Hz, 2H). ESI-MS: m/z 672.4 for $[M - PF_6]^+$. Anal. Calcd for $C_{37}H_{28}F_6N_7PRu$: C, 54.41; H, 3.46; N, 12.01. Found: C, 54.11; H, 3.42; N, 12.04.

Complex 3. To 10 mL of dry acetone were added Ru(tpy)Cl_3 (52 mg, 0.1 mmol) and AgOTf (78 mg, 0.3 mmol). The mixture was refluxed for 2 h before cooling to room temperature. The precipitate was removed by filtration, and the filtrate was concentrated to dryness. To the residue were added Mebib (33 mg, 0.1 mmol), DMF (8 mL), and *t*-BuOH (8 mL). The mixture then refluxed for 24 h. After cooling to room temperature, the solvent was removed under reduced pressure, and the residue was dissolved in the proper amount of methanol. After the addition of an excess of KPF_6, the resulting precipitate was collected by filtration and washing with water and Et_2O. The obtained solid was subjected to flash column chromatography on silica gel (eluent: 10:1 CH_2Cl_2/CH_3CN) to give 27 mg of complex **3** (33%). ^{1}H NMR (400 MHz, CD_3CN): δ 4.31 (s, 6H), 5.73 (d, J = 8.2 Hz, 2H), 6.76 (t,J = 7.7 Hz, 2H), 6.90 (t, J = 6.7 Hz, 2H), 7.08 (t, J = 7.6 Hz, 2H), 7.16 (d, J = 5.5 Hz, 2H), 7.38 (d, J = 8.3 Hz, 2H), 7.55 (m, overlapped, 3H), 8.31 (d, J = 7.9 Hz, 2H), 8.36 (t, J = 8.3 Hz, 1H), 8.41 (d, J = 7.8 Hz, 2H), 8.78 (d, J = 8.0 Hz, 2H). ESI-MS: m/z 672.3 for $[M - PF_6]^+$. Anal. Calcd for $C_{37}H_{28}F_6N_7PRu$: C, 54.41; H, 3.46; N, 12.01. Found: C, 54.25; H, 3.61; N, 12.03.

Complex 5. To 15 mL of ethylene glycol were added Mebip (84.8 mg, 0.25 mmol) and $RuCl_3{\cdot}3H_2O$ (32.6 mg, 0.125 mmol). The mixture was heated with microwave radiation (power 375 W) for 40 min. After cooling to room temperature, 10 mL of water and an excess of KPF_6 were added. The resulting precipitate was collected by filtration and washing with water and Et_2O. The obtained solid was subjected to flash column chromatography on silica gel (eluent: 200:5:1 acetone/H_2O/aqueous KNO_3) followed by anion exchange with KPF_6 to give 37 mg of complex **5** (28%). ^{1}H NMR (400 MHz, CD_3CN): δ 4.38 (s, 12H), 6.14 (d, J = 8.3 Hz, 4H), 6.99 (t, J = 7.8 Hz, 4H), 7.30 (t, J = 7.8 Hz, 4H), 7.47 (d, J = 8.3 Hz, 4H), 8.56 (t, J = 8.3 Hz, 2H), 8.89 (d, J = 8.2 Hz, 4H). ESI-MS: m/z 390.1 for $[M - 2PF_6]^{2+}$ (z = 2). Anal. Calcd for $C_{42}H_{34}F_{12}N_{10}P_2Ru{\cdot}2H_2O$: C, 45.62; H, 3.46; N, 12.67. Found: C, 45.28; H, 3.11; N, 12.80.

Complex 6. To 10 mL of dry acetone were added Ru(Mebip)Cl_3 (33.9 mg, 0.06 mmol) and AgOTf (78 mg, 0.3 mmol). The mixture was refluxed for 2 h before cooling to room temperature. The precipitate was removed by filtration, and the filtrate was concentrated to dryness. To the residue were added 2,2′:6′,2″-terpyridine (24 mg, 0.1 mmol) and 15 mL of ethylene glycol. The mixture was then heated with microwave radiation (P = 375 W) for 40 min. After cooling to room temperature, 10 mL of water and an excess of KPF_6 were added. The resulting precipitate was collected by filtration and washing with water and Et_2O. The obtained solid was subjected to flash column chromatography on silica gel (eluent: 200:5:1 CH_3CN/H_2O/aqueous KNO_3) followed by anion exchange with KPF_6 to give 30 mg of complex **6** (52%). ^{1}H NMR (400 MHz, CD_3CN): δ 4.40 (s, 6H), 5.97 (d, J = 8.3 Hz, 2H), 6.99 (t, J = 7.8 Hz, 2H), 7.12 (t, J = 6.6 Hz, 2H), 7.35 (m, overlapped, 4H), 7.58 (d, J = 8.4 Hz, 2H), 7.79 (t, J = 7.9 Hz, 2H), 8.41 (m, overlapped, 3H), 8.55 (t, J = 8.1 Hz, 1H), 8.78 (d, J = 8.3 Hz, 2H), 8.82 (d, J = 8.1 Hz, 2H). ESI-MS: m/z 336.9 for $[M - 2PF_6]^{2+}$ (z = 2). Anal. Calcd for $C_{36}H_{28}F_{12}N_8P_2Ru{\cdot}2H_2O$: C, 43.25; H, 3.23; N, 11.21. Found: C, 43.38; H, 3.12; N, 11,40.

Complex 8. A mixture of Ru(Mebip)Cl_3 (0.15 g, 0.27 mmol) and silver trifluoromethanesulfonate (AgOTf, 0.21 g, 0.82 mmol) was heated in 60 mL of acetone with stirring under light-protecting conditions for 2 h. After removal of the resulting AgCl precipitate by filtration, the solvent was evaporated. 4,6-Dimethyl-1,3-di-2-pyridylbenzene (Medpb, 95 mg, 0.41 mmol) and *n*-butanol (*n*-BuOH; 60 mL) were then added to the filtrate, and heating at 140 °C was continued for 15 h. After cooling to room temperature, the solvent was evaporated in vacuo. The brown residue was purified by column chromatography with CH_3CN/aqueous 0.5 M KNO_3 (9:1, v/v) as the eluent. The addition of a saturated KPF_6 aqueous solution to the main eluate resulted in precipitation of the product, which was collected by filtration. Purification by recrystallization from CH_3CN/water afforded 48 mg of complex **8** in a yield of 20%. ^{1}H NMR (500 MHz, DMSO-d_6): δ 4.15 (s, 6H), 4.48 (s, 6H), 5.95 (d, J = 8.6 Hz, 2H), 6.63 (t, J = 6.6 Hz, 2H), 6.85 (t, J = 7.4 Hz, 2H), 7.02 (d, J = 5.7 Hz, 2H), 7.19 (s, 1H), 7.21 (t, J = 7.7 Hz, 2H), 7.48 (t, J = 7.7 Hz, 2H), 7.67 (d, J = 8.6 Hz, 2H), 8.12 (d, J = 8.0 Hz, 2H), 8.31 (t, J = 8.2 Hz, 1H), 8.92 (d, J = 8.0 Hz, 2H). ESI-MS: m/z 700.284 for $[M - PF_6]^+$ (M = $C_{39}H_{32}N_7PF_6Ru$). Anal. Calcd for $C_{39}H_{32}N_7PF_6Ru$: C, 54.27; H, 3.97; N, 11.37. Found: 54.50; H, 4.00; N, 11.23. For X-ray crystallographic analysis, a BPh_4 salt of **8** was used instead of a PF_6 salt. [Ru(Mebip)(Medpb)](BPh_4) was easily obtained by anion exchange.

Complex 9. To 20 mL of dry *n*-BuOH were added complex **1** (93.8 mg, 0.1 mmol) and $AgBF_4$ (260 mg, 1.3 mmol). The mixture was refluxed for 5 h. After cooling to room temperature, the solvent was removed under reduced pressure and the residue was dissolved in the proper amount of methanol. After the addition of an excess of KPF_6, the resulting precipitate was collected by filtration and washing with water and Et_2O. The obtained solid was subjected to flash column

dx.doi.org/10.1021/ic2016885 | *Inorg. Chem.* 2012, 51, 890−899

chromatography on silica gel (eluent: 100:10:0.3 CH_3CN/H_2O/aqueous KNO_3) to give 60.9 mg of complex **9** (65%). This complex is paramagnetic because of the presence of ruthenium(III) species, as proved by the broadening of ^1H NMR signals. MALDI-TOF: m/z 778.1 for $[M - 2PF_6]^+$. Anal. Calcd for $C_{43}H_{34}F_{12}N_9P_2Ru \cdot C_4H_{10}O$: C, 49.43; H, 3.88; N, 11.04. Found: C, 49.37; H, 3.79; N, 11.23. The UV/vis absorption spectrum of complex **9** (Figure S7 in the Supporting Information) is virtually identical with that of one-electron-oxidized species of **1** recorded during spectroelectrochemical measurements (Figure 7a).

Electrochemical Measurements. All cyclic voltammograms were taken using a CHI620D potentiostat or an ALS/CHI model 660A electrochemical analyzer with a one-compartment electrochemical cell under an atmosphere of nitrogen. A glassy carbon electrode with a diameter of 0.3 mm was used as the working electrode. The electrode was polished prior to use with 0.05 μm alumina and rinsed thoroughly with water and acetone. A large-area platinum wire coil was used as the counter electrode. All potentials are referenced to a saturated Ag/AgCl electrode without regard for the liquid-junction potential. All measurements were carried out in acetonitrile at a scan rate of 100 mV/s, in 0.1 M of Bu_4NClO_4 (TBAP) as the supporting electrolyte.

Spectroscopic Measurements. UV/vis and near-IR (NIR) spectra were recorded on a TU-1810DSPC, Agilent 8453, or a Hitachi U-4000 UV/vis spectrophotometer at room temperature in acetonitrile, with a conventional 1 cm quartz cell. The emission spectra were recorded using a grating monochromator (Triax 1900, Jobin Yvon) with a CCD image sensor (S7031, Hamamatsu). The emission lifetime measurements were obtained by exciting deoxygenated samples with the Nd:YVO_4 laser, using the system previously described.[25]

Oxidative Spectroelectrochemistry. Oxidative spectroelectrochemistry was performed in a thin-layer cell (optical length = 0.05 cm) in which a platinum mesh working electrode was set. A platinum wire and $Ag/AgNO_3$ (0.01 M $AgNO_3$ in 0.1 M $TBAPF_6$ in CH_3CN) were used as a counter electrode and a reference electrode. The cell was put into the spectrometer to monitor the spectral change during electrolysis.

Computational Methods. DFT calculations are carried out using the B3LYP exchange correlation functional[26] and implemented in the *Gaussian 03* program package.[27] The electronic structures of complexes were determined using a general basis set with the Los Alamos effective core potential LanL2DZ basis set for ruthenium and 6-31G* for other atoms in the vacuum.[28]

X-ray Crystallography. A high-quality single crystal of [Ru(Mebip)(Medpb)](BPh_4) (red, needle) was mounted on a glass fiber and transferred into the cold nitrogen stream, and the X-ray diffraction data were collected using a Bruker SMART APEXII ULTRA CCD detector diffractometer on a rotating anode (Mo Kα radiation, graphite monochromator, λ = 0.710 73 Å). Corrections for absorption were made by *SADABS*.[29] The structure was solved by direct methods using *SHELXS-97* and refined anisotropically on F^2 with *SHELXL-97*.[30] All hydrogen atoms except those of water molecules were located in their idealized positions, with methyl C−H bond length 0.98 Å and aromatic C−H bond length 0.95 Å, and included in the refinement using a riding model approximation. The corresponding CIF file is available in the Supporting Information.

■ ASSOCIATED CONTENT

Supporting Information

Isodensity plots of frontier orbitals for complexes **2**, **3**, **5**, and **6**, Cartesian coordinates of all of the optimized geometries, TDDFT-predicted UV/vis spectra of complexes **1**−**3**, **5**, and **6**, absorption spectra of **1**, **8**, and **9**, NMR and MS spectra of new complexes, and a CIF file for complex **8**. This material is available free of charge via the Internet at http://pubs.acs.org.

■ AUTHOR INFORMATION

Corresponding Author

*E-mail: zhongyuwu@iccas.ac.cn (Y.-W.Z.), mhaga@kc.chuo-u.ac.jp (M.H.).

■ ACKNOWLEDGMENTS

Y.-W.Z. thanks the National Natural Science Foundation of China (Grant 21002104), the National Basic Research 973 program of China (Grant 2011CB932301), and Institute of Chemistry, Chinese Academy of Sciences ("100 Talent" Program), for funding support. M.H. is grateful for the partial financial support received from Chuo University Joint Research Grant 2009 and thanks the Ministry of Education, Culture, Sports, Science and Technology for a Grant-in-Aid for Priority Area "Coordination Programming" (Grant 21108003) and also for Scientific Research (Grant 21350082). We thank Prof. Koichi Nozaki at the University of Toyama for measuring the emission spectra and lifetimes.

■ REFERENCES

(1) (a) Schubert, U. S.; Eschbaumer, C. *Angew. Chem., Int. Ed.* **2002**, *41*, 2892. (b) Eryazici, I.; Moorefield, C. N.; Newkome, G. R. *Chem. Rev.* **2008**, *108*, 1834. (c) Medlycott, E. A.; Hanan, G. S. *Chem. Soc. Rev.* **2005**, *34*, 133. (d) Williams, J. A. G. *Chem. Soc. Rev.* **2009**, *38*, 1783.

(2) Hagfeldt, A.; Boschloo, G.; Sun, L.; Kloo, L.; Pettersson, H. *Chem. Rev.* **2010**, *110*, 6595.

(3) Ishida, H.; Tobita, S.; Hasegawa, Y.; Katoh, R.; Nozaki, K. *Coord. Chem. Rev.* **2010**, *254*, 2449.

(4) (a) Wenger, O. S. *Coord. Chem. Rev.* **2009**, *253*, 1439. (b) Hanss, D.; Walther, M. E.; Wenger, O. S. *Coord. Chem. Rev.* **2010**, *254*, 2584.

(5) (a) Constable, E. C. *Chem. Soc. Rev.* **2007**, *36*, 246. (b) Balzani, V.; Juris, A.; Venturi, M.; Campagna, S.; Serroni, S. *Chem. Rev.* **1996**, *96*, 759.

(6) (a) Ryabov, A. D.; Soukharev, V. S.; Alexandrova, L.; Lagadec, R. L.; Pfeffer, M. *Inorg. Chem.* **2003**, *42*, 6598. (b) Ceron-Camacho, R.; Morales-Morales, D.; Hernandez, S.; Lagadec, R. L.; Ryabov, A. D. *Inorg. Chem.* **2008**, *47*, 4988.

(7) (a) Djukic, J.-P.; Sortais, J.-B.; Barloy, L.; Pfeffer, M. *Eur. J. Inorg. Chem.* **2009**, 817. (b) Albrecht, M. *Chem. Rev.* **2010**, *110*, 576. (c) Wadman, S. H.; Havenith, R. W. A.; Hartl, F.; Lutz, M.; Spek, A. L.; van Klink, G. P. M.; van Koten, G. *Inorg. Chem.* **2009**, *48*, 5685. (d) Jäger, M.; Smeigh, A.; Lombeck, F.; Görls, H.; Collin, J.-P.; Sauvage, J.-P.; Hammarström, L.; Johannsson, O. *Inorg. Chem.* **2010**, *49*, 374. (e) Duprez, V.; Launay, J.-P.; Gourdon, A. *Inorg. Chim. Acta* **2003**, *343*, 395. (f) Moorlag, C.; Wolf, M. O.; Bohne, C.; Patrick, B. O. *J. Am. Chem. Soc.* **2005**, *127*, 6382.

(8) Wadman, S. H.; Lutz, M.; Tooke, D. M.; Spek, A. L.; Hartl, F.; Havenith, R. W. A.; van Klink, G. P.; van Koten, G. *Inorg. Chem.* **2009**, *48*, 1887.

(9) Arana, C. R.; Abruña, H. D. *Inorg. Chem.* **1993**, *32*, 194.

(10) (a) Duati, M.; Tasca, S.; Lynch, F. C.; Bohlen, H.; Vos, J. G.; Stagni, S.; Ward, M. D. *Inorg. Chem.* **2003**, *42*, 8377. (b) Duati, M.; Fanni, S.; Vos, J. G. *Inorg. Chem. Commun.* **2000**, *3*, 68.

(11) (a) Wadman, S. H.; Kroom, J. M.; Bakker, K.; Lutz, M.; Spek, A. L.; van Klink, G. P. M.; van Koten, G. *Chem. Commun.* **2007**, 1907. (b) Bessho, T.; Yoneda, E.; Yum, J.-H.; Guglielmi, M.; Tavernelli, I.; Imai, H.; Rothlisberger, U.; Nazeeruddin, M. K.; Gratzel, M. *J. Am. Chem. Soc.* **2009**, *131*, 5930. (c) Bomben, P. G.; Robson, K. C. D.; Sedach, P. A.; Berlinguette, C. P. *Inorg. Chem.* **2009**, *48*, 9631. (d) Koivisto, B. D.; Robson, K. C. D.; Berlinguette, C. P. *Inorg. Chem.* **2009**, *48*, 9644. (e) Bomben, P. G.; Koivisto, B. D.; Berlinguette, C. P. *Inorg. Chem.* **2010**, *49*, 4960. (f) Wadman, S. H.; Kroon, J. M.; Bakker, K.; Havenith, R. W. A.; van Klink, G. P. M.; van Koten, G. *Organometallics* **2010**, *29*, 1569. (g) Bomben, P. G.; Theriault, K. D.; Berlinguette, C. P. *Eur. J. Inorg. Chem.* **2011**, 1806. (h) Robson, K. C.

D.; Koivisto, B. D.; Yella, A.; Sporinova, B.; Nazeeruddin, M. K.; Baumgartner, T.; Gratzel, M.; Berlinguette, C. P. *Inorg. Chem.* **2011**, *50*, 5494.
(12) (a) Patoux, C.; Launay, J.-P.; Beley, M.; Chodorowski-Kimmers, S.; Collin, J.-P.; James, S.; Sauvage, J.-P. *J. Am. Chem. Soc.* **1998**, *120*, 3717. (b) Fraysse, S.; Coudret, C.; Launay, J.-P. *J. Am. Chem. Soc.* **2003**, *125*, 5880. (c) Steenwinkel, P.; Grove, D. M.; Veldman, N.; Spek, A. L.; van Koten, G. *Organometallics* **1998**, *17*, 5647. (d) Gagliardo, M.; Amijs, C. H. M.; Lutz, M.; Spek, A. L.; Havenith, R. W. A.; Hartl, F.; van Klink, G. P. M.; van Koten, G. *Inorg. Chem.* **2007**, *46*, 11133. (e) Yao, C.-J.; Sui, L.-Z.; Xie, H.-Y.; Xiao, W.-J.; Zhong, Y.-W.; Yao, J. *Inorg. Chem.* **2010**, *49*, 8347. (f) Vila, N.; Zhong, Y.-W.; Henderson, J. C.; Abruña, H. D. *Inorg. Chem.* **2010**, *49*, 796. (g) Wang, L.; Yang, W.-W.; Zheng, R.-H.; Shi, Q.; Zhong, Y.-W.; Yao, J. *Inorg. Chem.* **2011**, *50*, 7074. (h) Yao, C.-J.; Zhong, Y.-W.; Yao, J. *J. Am. Chem. Soc.* **2011**, *133*, 15697.
(13) (a) Zhong, Y.-W.; Wu, S.-H.; Burkhardt, S. E.; Yao, C.-J.; Abruña, H. D. *Inorg. Chem.* **2011**, *50*, 517. (b) Wu, S.-H.; Burkhardt, S. E.; Yao, J.; Zhong, Y.-W.; Abruña, H. D. *Inorg. Chem.* **2011**, *50*, 3959.
(14) Yang, W.-W.; Wang, L.; Zhong, Y.-W.; Yao, J. *Organometallics* **2011**, *30*, 2236.
(15) (a) Haga, M.; Kobayashi, K.; Terada, K. *Coord. Chem. Rev.* **2007**, *251*, 2688. (b) Haga, M.; Takasugi, T.; Tomie, A.; Ishizuya, M.; Yamada, T.; Hossain, M. D.; Inoue, M. *Dalton Trans.* **2003**, 2069. (c) Terada, K.; Kobayashi, K.; Haga, M. *Dalton Trans.* **2008**, 4846. (d) Ashizawa, M.; Yang, L.; Kobayashi, K.; Sato, H.; Yamagishi, A.; Okuda, F.; Harada, T.; Kuroda, R.; Haga, M. *Dalton Trans.* **2009**, 1700. (e) Haga, M.; Hong, H.-G.; Shiozawa, Y.; Kawata, Y.; Monjushiro, H.; Fukuo, T.; Arakawa, R. *Inorg. Chem.* **2000**, *39*, 4566. (f) Yutaka, T.; Obara, S.; Ogawa, S.; Nozaki, K.; Ikeda, N.; Ohno, T.; Ishii, Y.; Sakai, K.; Haga, M. *Inorg. Chem.* **2005**, *44*, 4737. (g) Obara, S.; Itabashi, M.; Okuda, F.; Tamaki, S.; Tanabe, Y.; Ishii, Y.; Nozaki, K.; Haga, M. *Inorg. Chem.* **2006**, *45*, 8907. (h) Terada, K.; Kanaizuka, K.; Iyer, V. M.; Sannodo, M.; Saito, S.; Kobayashi, K.; Haga, M.-a. *Angew. Chem., Int. Ed.* **2011**, *50*, 6287.
(16) (a) Ruttimann, S.; Bernardinelli, G.; Williams, A. F. *Angew. Chem., Int. Ed.* **1993**, *32*, 392. (b) Carina, R. F.; Williams, A. F.; Bernardinelli, G. *Inorg. Chem.* **2001**, *40*, 1826.
(17) Piguet, C.; Bernardinelli, G.; Williams, A. F. *Inorg. Chem.* **1989**, *28*, 2920.
(18) (a) Tam, A. Y.-Y.; Lam, W. H.; Wong, K. M.-C.; Zhu, N.; Yam, V. W.-W. *Chem.—Eur. J.* **2008**, *14*, 4562. (b) Mathew, I.; Sun, W. *Dalton Trans.* **2010**, *39*, 5885. (c) Wang, K.; Haga, M.; Monjushiro, H.; Akiba, M.; Sasaki, Y. *Inorg. Chem.* **2000**, *39*, 4022.
(19) (a) Chandrashekhar, N.; Gayathri, V.; Gowda, N. M. N. *Polyhedron* **2010**, *29*, 288. (b) Gayathri, V.; Leelamani, E. G.; Gowda, N. M. N.; Reddy, G. K. N. *Polyhedron* **1999**, *18*, 2351.
(20) (a) Terazzi, E.; Guenee, L.; Morgantini, P.-Y.; Bernardinelli, G.; Donnio, B.; Guillon, D.; Piguet, C. *Chem.—Eur. J.* **2007**, *13*, 1674. (b) Terazzi, E.; Torelli, S.; Bernardinelli, G.; Rivera, J.-P.; Benech, J.-M.; Bourgogne, C.; Donnio, B.; Guillon, D.; Imbert, D.; Bunzli, J.-C. G.; Pinto, A.; Jeannerat, D.; Piguet, C. *J. Am. Chem. Soc.* **2005**, *127*, 888.
(21) (a) Kohle, O.; Ruile, S.; Gratzel, M. *Inorg. Chem.* **1996**, *35*, 4799. (b) Concepcion, J. J.; Tsai, M.-K.; Muckerman, J. T.; Meyer, T. J. *J. Am. Chem. Soc.* **2010**, *132*, 1545. (c) Chen, Z.; Concepcion, J. J.; Luo, H.; Hull, J. F.; Paul, A.; Meyer, T. J. *J. Am. Chem. Soc.* **2010**, *132*, 17670. (d) Concepcion, J. J.; Jurss, J. W.; Brennaman, M. K.; Hoertz, P. G.; Patrocinio, A. O. T.; Iha, N. Y. M.; Templeton, J. L.; Meyer, T. J. *Acc. Chem. Res.* **2009**, *42*, 1954.
(22) Xiao, X.; Haga, M.; Matsumura-Inoue, T.; Ru, Y.; Addison, A. W.; Kano, K. *J. Chem. Soc., Dalton Trans.* **1993**, 2477.
(23) (a) Lever, A. B. P. *Inorg. Chem.* **1990**, *29*, 1271. (b) Masui, H.; Lever, A. B. P. *Inorg. Chem.* **1993**, *32*, 2199. (c) Lever, A. B. P.; Dodsworth, E. S. In *Comprehensive Coordination Chemistry II*; Lever, A. B. P., Ed.; Elsevier Publishers: New York, 2004; Vol. 2, pp 251−268.
(24) Seok, W. K.; Meyer, T. J. *Inorg. Chem.* **2005**, *44*, 3931 and references cited therein.
(25) Yang, L.; Okuda, F.; Kobayashi, K.; Nozaki, K.; Tanabe, Y.; Ishii, Y.; Haga, M.-a. *Inorg. Chem.* **2008**, *47*, 7154.
(26) (a) Becke, A. D. *J. Chem. Phys.* **1993**, *98*, 5648. (b) Lee, C.; Yang, W.; Parr, R. G. *Phys. Rev. B* **1988**, *37*, 785.
(27) Frisch, M. J.; Trucks, G. W.; Schlegel, H. B.; Scuseria, G. E.; Robb, M. A.; Cheeseman, J. R.; Montgomery, J. A., Jr.; Vreven, T.; Kudin, K. N.; Burant, J. C.; Millam, J. M.; Iyengar, S. S.; Tomasi, J.; Barone, V.; Mennucci, B.; Cossi, M.; Scalmani, G.; Rega, N.; Petersson, G. A.; Nakatsuji, H.; Hada, M.; Ehara, M.; Toyota, K.; Fukuda, R.; Hasegawa, J.; Ishida, M.; Nakajima, T.; Honda, Y.; Kitao, O.; Nakai, H.; Klene, M.; Li, X.; Knox, J. E.; Hratchian, H. P.; Cross, J. B.; Adamo, C.; Jaramillo, J.; Gomperts, R.; Stratmann, R. E.; Yazyev, O.; Austin, A. J.; Cammi, R.; Pomelli, C.; Ochterski, J. W.; Ayala, P. Y.; Morokuma, K.; Voth, G. A.; Salvador, P.; Dannenberg, J. J.; Zakrzewski, V. G.; Dapprich, S.; Daniels, A. D.; Strain, M. C.; Farkas, O.; Malick, D. K.; Rabuck, A. D.; Raghavachari, K.; Foresman, J. B.; Ortiz, J. V.; Cui, Q.; Baboul, A. G.; Clifford, S.; Cioslowski, J.; Stefanov, B. B.; Liu, G.; Liashenko, A.; Piskorz, P.; Komaromi, I.; Martin, R. L.; Fox, D. J.; Keith, T.; Al-Laham, M. A.; Peng, C. Y.; Nanayakkara, A.; Challacombe, M.; Gill, P. M. W.; Johnson, B.; Chen, W.; Wong, M. W.; Gonzalez, C.; Pople, J. A. *Gaussian 03*, revision E.01; Gaussian Inc.: Pittsburgh, PA, 2007.
(28) (a) Dunning, T. H.; Hay, P. J. In *Modern Theoretical Chemistry*; Schaefer, H. F., Ed.; Plenum: New York, 1976; Vol. 3, p 1. (b) Hay, P. J.; Wadt, W. R. *J. Chem. Phys.* **1985**, *82*, 270. (c) Wadt, W. R.; Hay, P. J. *J. Chem. Phys.* **1985**, *82*, 284. (d) Hay, P. J.; Wadt, W. R. *J. Chem. Phys.* **1985**, *82*, 299.
(29) Sheldrick, G. M. *SADABS*; Bruker AXS Inc.: Madison, WI, 1997.
(30) Sheldrick, G. M. *SHELXS97 and SHELXL97*; University of Göttingen: Göttingen, Germany, 1997.